Uncertainty Visualization in Forward and Inverse Cardiac Models

Brett M Burton[12], Burak Erem[4], Kristin Potter[1], Paul Rosen[1], Chris R Johnson[1], Dana H Brooks[3], Rob S Macleod[1,2]

[1]Scientific Computing and Imaging Institute, University of Utah, Salt Lake City, Utah, USA
[2]Bioengineering Department, University of Utah.
[3]Department of Electrical and Computer Engineering, Northeastern University, Boston, MA, USA
[4]Computational Radiology Laboratory, Children's Hospital, Boston, MA, USA

Abstract

Quantification and visualization of uncertainty in cardiac forward and inverse problems with complex geometries is subject to various challenges. Specific to visualization is the observation that occlusion and clutter obscure important regions of interest, making visual assessment difficult. In order to overcome these limitations in uncertainty visualization, we have developed and implemented a collection of novel approaches. To highlight the utility of these techniques, we evaluated the uncertainty associated with two examples of modeling myocardial activity. In one case we studied cardiac potentials during the repolarization phase as a function of variability in tissue conductivities of the ischemic heart (forward case). In a second case, we evaluated uncertainty in reconstructed activation times on the epicardium resulting from variation in the control parameter of Tikhonov regularization (inverse case). To overcome difficulties associated with uncertainty visualization, we implemented linked-view windows and interactive animation to the two respective cases. Through dimensionality reduction and superimposed mean and standard deviation measures over time, we were able to display key features in large ensembles of data and highlight regions of interest where elevated uncertainties exist.

1. Introduction

Forward and inverse problems in electrocardiography provide a means for studying the electrical properties and patterns that arise within the heart and/or torso from the integrated electrical activity of cardiac myocytes. In the forward case, electrical inferences are made based on given source models and associated conducting media that contain these sources. Inverse solutions, in contrast, use remote observations to deduce the electrical function of the cardiac sources. Solutions to forward and inverse problems, however, require assumptions that, due to such characteristics as the complex nature of cardiac structure or the inherent need to regularize the inverse, generate uncertainty in the results.

To understand the uncertainty associated with cardiac forward and inverse problems, visualization techniques are often applied; however, visualization of *3-dimensional* data presents its own set of complexities. Obstruction and clutter can obscure or even hide regions of interest. To overcome these difficulties in visualization and thus to better understand variations in the uncertainty of electrocardiographic models, we have developed new *3-dimensional* techniques to visually analyze simulation uncertainty.

In order to explore uncertainty visualization, we considered two electrocardiographic simulation cases—one for forward and one for inverse simulation. We first investigated the uncertainty associated with bidomain conductivities in the static forward model of an ischemic heart. In the second case, we explored variability in reconstructed activation times, computed by way of Tikhonov inverse, as a function of the regularization parameter, λ. To investigate the uncertainties in our models, we have developed—and present here—new visualization systems that overcome many of the difficulties of *3-dimensional* rendering and support interactive exploration of high-dimensional uncertainty.

2. Methods

While both forward and inverse problems in electrocardiography seek to capture electric activity from the heart, they are different in formulation and solution approach. Each, therefore, required unique and specific uncertainty quantification and visualization approaches.

2.1. Static Ischemic Forward Model

To generate data for the static ischemia model, we extracted heart and ischemic zone geometries from experimentally induced ischemic studies using approaches de-

Table 1. Ratios applied to tensor conductivity values within the ischemic region to simulate the diseased state.

Conductivity	Ischemic Ratio
σ_{il}	1/10
σ_{it}	1/1000
σ_{el}	1/2
σ_{et}	1/4

scribed previously [1, 2]. Fiber directions, acquired by diffusion tensor imaging (DTI), were also assigned.

In order to simulate ischemia, anisotropic conductivity values within the ischemic region were decreased (see Table 1) and a potential difference of 30 mV was applied to the transmembrane potential, V_m, to represent the weakened activity during the plateau phase (which corresponds to the ST segment of the ECG) of the ischemic action potential[3]. The model also included a linear transition region (border zone) from the diseased to healthy tissue [4].

Cardiac activity under these conditions was represented by the bidomain passive current flow equation [3]

$$\nabla \cdot (\overline{\sigma}_i + \overline{\sigma}_e)\nabla V_e = -\nabla \cdot \overline{\sigma}_i \nabla V_m, \quad (1)$$

where $\overline{\sigma}_i$ and $\overline{\sigma}_e$ represent the intracellular and extracellular conductivity tensors, respectively, and V_e represents the unknown extracellular potentials.

There have been many studies attempting to document the conductivity values of the heart [5, 6]; however, these values remain elusive and, therefore, provide a source of uncertainty for the model. We selected a range of conductivity values from the literature [7] onto which we applied generalized polynomial chaos-stochastic collocation methods (gPC-SC) [8]. Conductivity values were treated as uniformly distributed, stochastic processes within the conductivity range provided. gPC-SC was used to reduce the stochastic governing equations into a finite set of deterministic simulation parameters, reducing computational complexity and allowing us to extract the mean and probability density function of the resulting solution ensemble.

2.2. Activation Time Inverse Solutions

The activation-based inverse problem aims to estimate the spread of electrical activation over the epicardium from measurements of electric potentials on the body surface during the QRS complex. In order to provide validation data, the body surface potentials were generated by solving a forward model distinct from the one described in the previous section. This forward model was composed of a nonlinear function, $x(\tau)$, which mapped a set of activation times to transmembrane potentials (TMPs) from a discrete set of electrical sources on an artificially constructed, combined epicardial and endocardial surface[**?**], and a linear mapping, A, a matrix that computes body surface potentials from TMPs. The resulting inverse problem is not only non-linear but also ill-conditioned and hence requires regularization. A simple, yet effective approach to regularization uses the Tikhonov [9] method, resulting in the following non-linear, least squares (NLLS) optimization problem, which is non-convex [10]:

$$\tau_\lambda = argmin \|Ax_\tau - b\|^2_{Frob} + \lambda \|Lx_\tau\|^2_{Frob}, \quad (2)$$

where b are the body surface potentials, L is a regularization matrix, and λ is a regularization parameter that controls the trade-off between data fidelity and solution smoothness.

We have previously used a convex relaxation of the above problem and discovered uncertainty in the solutions, possibly due, in part, to the inherent sensitivity of the problem to signal noise, geometric errors, forward model assumptions (*e.g.* source amplitudes), and inverse problem parameters (*e.g.* L and λ) [10, 11]. In this study, we focused on the uncertainty generated by the selection of λ. We chose 50 evenly-spaced values within the interval $[0.09, 0.11]$ on which we performed a perturbation analysis. For each λ, a solution was found for the convex relaxation, from which activation times were computed; from these values, we calculated statistics of the activation time (mean and standard deviation) for each source on the heart surface. This spatial distribution of mean and standard deviation of the activation time gave a measure of the uncertainty of the solution associated with λ selection.

2.3. μView: Myocardial Uncertainty Viewer

To enable uncertainty visualization for the volumetric ischemic simulations we created a five-way, linked-view tool (μView), examples of which are shown in Figure 1. We then combined simulation results acquired in Section 2.1 and applied a dimensionality reduction approach to provide a means of displaying large ensembles of high dimensional data. Figures 1A and 1B show standard deviations and isovalue separation, respectively, as two forms of dimensionality reduction for visualization. Other methods were also employed to explore the data including: mean, minimum and maximum isosurfaces, and clustering based on several correlation metrics. Mean and standard deviation visualizations applied simple statistical measures at each node of the simulation with increased intensity representing increased values. Isovalue separation scanned each node of the simulation set and determined how many nodes were above (red) and below (blue) the assigned isovalue. [The spectrum of color between these two extrema reflected nodes that had values, within the solution ensemble, that were both above and below the threshold. —¡I

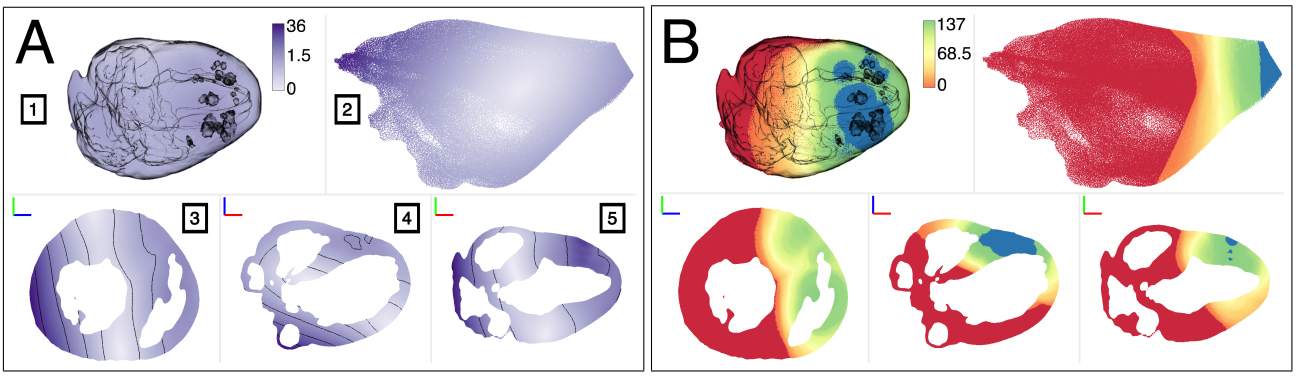

Figure 1. Uncertainty Visualization of the Cardiac Ischemia Forward Model. (A) Standard deviation and (B) isolvalue rendering of cardiac forward model show regions of interest near the ischemic zone (outlined in pane 1). The five-way linked view contains the following viewing modalities: 1 volumetric, 2 2*D* parameter space, 3 - 5 *2D* slicing planes.

cannot picture this. If red and blue are the extremes, then colors between these extreme should map to the points between the extremes but what does this have to do with a threshold?¿] [Minimum and maximum isosurfaces use the isovalue results to highlight only the surfaces produced by the isovalue extrema. —¡Again, I really have a hard time picturing what you mean with this description?¿] Clustering applied k-means methods to bin similar nodes together, with L2 norm, Pearson's correlation, or histogram difference used as similarity metrics.

To overcome difficulties associated with *3D* rendering we used the following visual techniques: volume rendering (Figure 1A 1), a *2D* view of parameter space (2) and three orthogonal *2D* slicing planes (panes 3 – 5). Volume rendering and *2D* slicing planes are standard visualization techniques used in this case to display data values at each point within the myocardium. The parameter space view, in order to reduce the high dimensional data while preserving important features, uses principle component analysis to contract the solution space into a *2D* representation—allowing the user to explore features not otherwise visible in the spatial domain. The shape of the resulting image is arbitrary and is a result of the selected principle components. For more information on the technical aspects of these methods, please see our prior publications [12].

2.4. Uncertainty Animation

Static isochronal maps of activation times are the most common visualization method for activation-based simulations of the spread of excitation in the heart. Such compression of an entire heart beat into a single image is one of the advantages of activation mapping that supports its utility in research and clinical applications. However, in the setting of visualizing uncertainty, the need to view additional parameters and their variation over both time and parameter space provides new challenges. To address this challenge, we have expanded the static, single image of activation to become an interactive animation over time. Similar to visualizing an animation of the moving activation wavefront, each frame of our animation shows spatial regions that are within one standard deviation of the current mean activation time and allows the user to move forward and backward in time as well as adjust view parameters. Figure 2 shows a single time instant from such an animation in which regions in yellow correspond to areas with low standard deviation values, *i.e.,* represent the mean activation time values. Other regions, spanning from red to purple, display larger values of the standard deviation and indicate the spatial distributions of uncertainty for this particular time instant. Examples of this uncertainty animation can be found at `http://www.sci.utah.edu/~kpotter/research/heartActivation/`

3. Results

Visualizing the results of varied conductivity parameters in the forward problem and the regularization parameter of the inverse problem allowed us to identify regions of interest within simulation results. In the ischemic forward model, isosurfacing, min/max isosurfacing, and clustering allowed us to identify regions [—of high uncertainty ¡Is this what you mean? not clear as it stands now¿] near the ischemic zone [by scanning the solution space of the simulation—¡This seems repetitive and not clearly useful¿]. Though independent of the physical space, these methods were able to scan the solution space and provide the viewer with a sense of uncertainty with respect to a specified isovalue or number of bins. By projecting these findings onto the physical space we were able to observe at what location, the chosen solution parameters differed. Standard deviation values were able to illustrate regions of uncertainty, within the areas of interest, as a [sense of—] a range of variance within the solution ensemble.

By animating the activation based inverse solution, we were able to identify regions on the surface of the heart that exhibited higher temporal and spatial uncertainty. During a single frame of the animation ([such as is seen in — *e.g.,*] Figure 2) the standard deviation in some regions span[—ned] a small distance (1/10 of the LV circumference) where[—as] other regions show[—ed] spatial variation as large as 1/4 of the LV circumference. The temporal discrepancy in activation times within these spatial regions [is—was] as high as 36.4 ms.

3.1. Discussion

By using several uncertainty visualization techniques, we were able to highlight regions of interest in ischemic forward simulations and activation-based inverse solutions. Questions stemming from discrepancies in experimentally measured conductivity values for cardiac tissue generated small uncertainties in the forward solution. Regions in or near the ischemic region exhibited greater standard deviations, while regions near the epicardium (where DTI-defined fiber directions exhibited more random directional behavior) had wider discrepancies between min and max isosurfaces (not shown). These results remain inconclusive and will require further investigation. Likewise, for the inverse case, spatial regions were shown to exhibit higher standard deviations than others based on different, user selected regularization parameters, λ, that merits additional study.

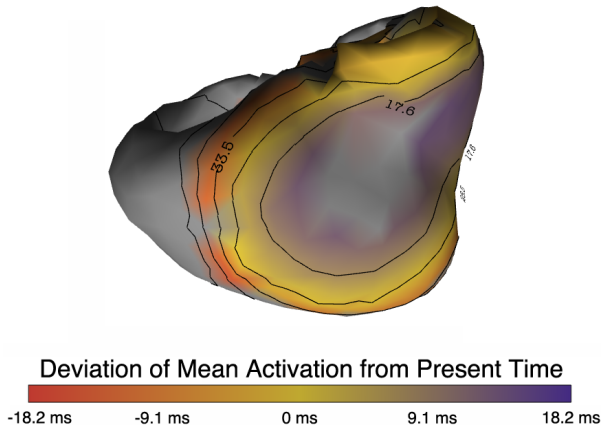

Figure 2. Spatial Distribution of Activation Times and Standard Deviations. Animations of uncertainty in the spatial distribution of activation times on heart surfaces at 30 ms. Color maps show the spatial location and the difference between the present time and the mean activation time (within one standard deviation).

Acknowledgements

This project was supported by grants from the National Center for Research Resources (5P41RR012553-14) and the National Institute of General Medical Sciences (8 P41 GM103545-14) from the National Institutes of Health and by Award No. KUS-C1-016-04, made by King Abdullah University of Science and Technology (KAUST). Experiment data collection was funded by the Nora Eccles Treadwell Foundation at the Cardiovascular Research and Training Institute.

References

[1] Shome S, MacLeod R. Simultaneous high-resolution electrical imaging of endocardial, epicardial and torso-tank surfaces under varying cardiac metabolic load and coronary flow. In Functional Imaging and Modeling of the Heart, Lecture Notes in Computer Science 4466. Springer-Verlag, 2007; 320–329.

[2] Aras K, Shome S, Swenson D, Stinstra J, MacLeod R. Electrocardiographic response of the heart to myocardial ischemia. In Computers in Cardiology 2009. 2009; 105–108.

[3] Hopenfeld B, Stinstra J, MacLeod R. Mechanism for ST depression associated with contiguous subendocardial ischemia 2004;15(10):1200–1206.

[4] Swenson D, Stinstra J, Burton B, Aras K, Healy L, , MacLeod R. Evaluating the effects of border zone approximations with subject specific ischemia models. In Doessel O, Schlegel WC (eds.), World Congress on Med. Phys. and Biomed. Eng., volume 25/IV. Heidelberg: Springer, 2009; 1680–1683.

[5] Plonsey R, Barr R. A critique of impedance measurements in cardiac tissue 1986;14:307–322.

[6] Pollard A, Barr R. A biophysical model for cardiac microimpedance measurements. Jun 2010;298(6):H1699–H1709.

[7] Johnston P, Kilpatrick D. The effect of conductivity values on ST segment shift in subendocardial ischaemia 2003; 50(2):150–158.

[8] Xiu D. Efficient collocational approach for parametric uncertainty analysis. Comm Comp Phys 2007;2:293–309.

[9] Tikhonov A, Arsenin V. Solution of Ill-posed Problems. Washington, DC: Winston, 1977.

[10] Erem B, van Dam P, Brooks D. A convex relaxation framework for initialization of activation-based inverse electrocardiography. In NFSI & ICBEM 8th International Symposium on IEEE, 2011. 2011; .

[11] Erem B, van Dam P, Brooks D. Analysis of the criteria of activation-based inverse electrocardiography using convex optimization. In Conf Proc IEEE Eng Med Biol Soc. 2011; .

[12] Rosen P, Burton B, Potter K, Johnson CR. Visualization for understanding uncertainty in the simulation of myocardial ischemia. In The 3rd International Workshop on Visualization in Medicine and Life Sciences. 2013; .